

An Investigation of Electrostatic Probe Perturbations on the Operational Characteristics of a Hall Thruster and on the Measurement of Local Plasma Parameters

James M. Haas^{*}, Gregory G. Spanjers[‡], Keith McFall^{*}, Ronald A. Spores[§]
 Air Force Research Laboratory - Propulsion Directorate
 Electric Propulsion Lab
 Edwards AFB, CA

ABSTRACT

A high speed reciprocating probe system was constructed and used to investigate the perturbations of electrostatic probes on Hall thruster operations and on the measurement of local plasma parameters. Two regimes were investigated: inside the discharge chamber where the probe actively burned and at the exit plane where the probe experienced significant particle flux without burning. Experiments showed that in the interior of the thruster, significant probe material ablation occurred and severe perturbations to thruster operation and plasma measurements could not be avoided, even with residence times as short as 0.5 s. At the exit plane of the thruster, no material ablation was observed, however, significant variations of the local measurements of electron temperature and number density were observed. Measurement variations were successfully avoided by the use of the high-speed probe, which kept the probe residence time to less than 0.5 s.

NOMENCLATURE

A_j	Current collection area of electrode j	t	Melting time
A	Power loading area	T_{\max}	Melting temperature
C_p	Specific heat	V_j	Potential of electrode j
e	Electron charge	V_f	Floating potential
f	Particle flux	V_p	Plasma potential
I_e	Electron current	ΔV	Probe bias
I_i	Ion current	v	Particle velocity
J_i	Ion current density	λ_d	Debye length
K	Kinetic energy	ρ	Material density
k_b	Boltzmann constant	C_{dj}	Nondimensional potential difference between electrode j and electrode 1
k_{th}	Thermal conductivity		
l	Probe length		
m_e	Electron mass		
m_i	Ion mass		
n_e	Electron number density		
P	Power to probe		
r	Probe radius		
T_e	Electron temperature		
T_i	Ion temperature		

INTRODUCTION

Electrostatic (or Langmuir) probes are among the simplest and most commonly used plasma diagnostic tools. Their use dates back to Langmuir's[1] original development of the theory to describe probe behavior in a plasma. Since that time electrostatic probes have found use in a wide range of disciplines ranging from nuclear fusion[2] to atmospheric and space sciences[3]. In particular, they have been used

^{*} Research Aerospace Engineer, AFRL Electric Propulsion Laboratory, Member AIAA

[‡] Group Leader, AFRL Electric Propulsion Laboratory, Member AIAA

[§] Chief, Spacecraft Propulsion Branch, Member AIAA

This paper is declared a work of the US government and is not subject to copyright protection in the United States

extensively in the field of electric propulsion to provide a relatively simple means of measuring electron temperature, electron number density, plasma potential and floating potential. Electrostatic probes have been used in single, double, triple and quadruple configurations in a number of devices including arcjets, Lorentz Force Accelerators, ion engines and Hall thrusters[4-10].

A great deal of analysis has been done[10] to determine probe measurement uncertainty resulting from the deviation of the measured voltage/current characteristic from that predicted by theory. However, there has been relatively little investigation of the effect the probe itself has on the surrounding plasma and hence on the quantities it is attempting to measure. In plasmas with highly energetic charged particles, probe material is generally sputtered and/or ablated by direct plasma flux. Local plasma temperature and density is then affected through emission of relatively cold probe material. These perturbations may remain localized near the probe, or may propagate further into the plasma depending upon the various collisional mean free path lengths.

In very high temperature and density plasmas, such as nuclear fusion devices, probe lifetimes on the order of milliseconds drove the need to develop high speed reciprocating probe systems[2]. In the case of Hall thrusters, for measurements downstream of the exit plane, probe lifetime requirements are not as rigorous. However, within the discharge chamber, plasma temperature and density increase, probe heating increases significantly, and probe survival times are shortened. Under these conditions, a high speed, reciprocating probe system can minimize these effects, allowing for more accurate measurements of local plasma parameters.

An electrostatic probe and high speed, reciprocating positioning system were constructed to investigate perturbations to the plasma of a Hall thruster. The following sections describe the experimental techniques and apparatus, present experimental results, and discuss the implications of these results.

THEORY

A simple model was developed to predict the thermal evolution of a probe in the plume of a Hall thruster. The probe was modeled as a cylinder with radius, r , and length, l , and it was assumed that all probe heating resulted from direct particle flux to the

surface. The power to the probe consisted of four components:

1. Directed ion power to the probe end

$$P_i^d = f_i^d K_i^d A_i^d \quad (1)$$

where

$$f_i^d = n_e v_i^d \quad (2)$$

$$K_i^d = \frac{1}{2} m_i (v_i^d)^2 \quad (3)$$

$$A_i^d = \pi r^2 \quad (4)$$

2. Bohm ion power to probe sides

$$P_i^b = f_i^b K_i^b A_i^b \quad (5)$$

where

$$f_i^b = n_{e0} v_i^b \quad (6)$$

$$v_i^b = \sqrt{\frac{k_b T_e}{m_i}} \text{EXP}\left[-\frac{1}{2}\right] \quad (7)$$

$$K_i^b = \frac{1}{2} m_i (v_i^b)^2 \quad (8)$$

$$A_i^b = 2\pi r l \quad (9)$$

3. Electron thermal power

$$P_e = f_e K_e A_e \quad (10)$$

where

$$f_e = \frac{1}{4} n_e v_e \quad (11)$$

$$n_e = n_{e0} \text{EXP} \left[\frac{e(V_f - V_p + \Delta V)}{k_b T_e} \right] \quad (12)$$

$$v_e = \sqrt{\frac{8k_b T_e}{pm_e}} \quad (13)$$

$$K_e = \frac{1}{2} m_e v_e^2 \quad (14)$$

$$V_f = V_p + \frac{k_b T_{ev}}{e} * \text{Log} \left(\sqrt{\frac{2pm_e}{m_i}} \text{Exp} \left[-\frac{1}{2} \right] A_e + v_i^d A_i^d \sqrt{\frac{2pm_e}{k_b T_{ev}}} \right) \quad (15)$$

4. Hall current power

$$P_{ExB} = K_{ExB} f_{ExB} = \frac{1}{2} m_e n_e v_{ExB}^3 \quad (16)$$

where

$$v_{ExB} = \frac{E}{B} \quad (17)$$

For the case of the directed ion flux to the probe tip, it was necessary to include axial heat conduction along the length of the probe. Using a standard, 1D, semi-infinite plane approach, the time to reach a given temperature at the probe tip can be written

$$t_{tip} = 2 \frac{P_i^d}{A_i^d} \sqrt{\frac{T_{max}}{prC_p k_{th}}} \quad (18)$$

For the ion Bohm, electron and Hall current heating, a bulk heating approach assuming no axial or radial transport is sufficient. The time to reach a given bulk temperature is then written

$$t_{bulk} = \frac{1}{2} r r C_p T_{max} \left(\frac{A_{i,e}^b}{P_{i,e}^b} \right) \quad (19)$$

Combining the individual heating components, the probe melting time can be estimated as a function of electron temperature and number density. Omitting the Hall current, directed ion flux dominates, yielding tungsten and alumina burning times on the order of 4000 s and 300 s, respectively. Using representative values of $E=1E5V/m$ and $B=400G$, the addition of the Hall current reduces the burning time to several hundred milliseconds.

EXPERIMENTAL APPARATI AND TECHNIQUES

Chamber

All tests were conducted in Chamber 6 at the Air Force

Research Laboratory's Electric Propulsion Lab at Edwards Air Force Base, CA. The 5'x8' vacuum facility is evacuated by a single Stokes mechanical pump and blower, 4 copper cryopanel maintained at 25 K by 4 APD cold heads and model HC-8C helium compressors, and an APD 22" cryopump. Heat load to the cryopanel is minimized by a pair of copper shrouds coated with low emissivity paint and chilled by a TM refrigeration unit. This configuration yields a total pumping speed of 26,000 l/s of xenon and a base pressure of 9×10^{-7} Torr. A MKS Model 919 Hot Cathode Ionization Gauge monitored the background chamber pressure, which was maintained below 5×10^{-5} Torr during all tests. Figure 1 illustrates the layout of Chamber 6.

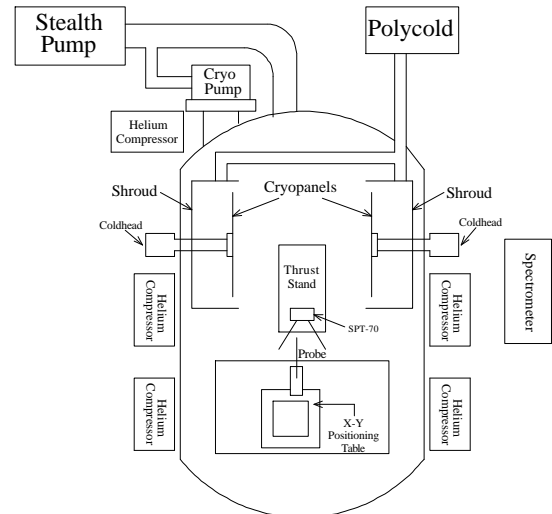


Figure 1. Air Force Research Laboratory Chamber 6 Layout

Thruster

A Fakel SPT-70 was used for all experiments. This thruster was designed to operate at 660 W nominal discharge power yielding 40 mN of thrust and 1500 s I_{sp} at 40% efficiency. For all tests the SPT-70 was operated at 300 V, 2.2 A and 26 sccm of xenon, 3 sccm of which was supplied to the cathode.

Propellant flow to the thruster was controlled by an array of Unit Model 8100 mass flow controllers, calibrated for xenon. Flow system components and tubing were cleaned and electropolished to a 10 Ra finish and all connections were welded. System leak rates were determined to be less than 1×10^{-7} sccm. Flow rates were calibrated by comparison to flow into a known volume.

Spectrometer

A SPEX 1m spectrometer with a 1200 G/mm, 11 cm, first order grating was used during a portion of the experiment to detect species from the burning tungsten electrode and alumina insulation. The tip of the probe at the exit plane of the thruster was imaged onto the entrance slit of the spectrometer using a 600 mm focal length, 3-inch lens. A pair of telescoping mirrors rotated the probe image, aligning the axis of the probe along the slit. Output was collected by a Hamamatsu 921 photomultiplier tube and recorded on a TEK TDS460 oscilloscope. The entrance and exit slit widths were both 50 μm providing a resolution of about 0.3 \AA .

In-situ calibration of the spectrometer was accomplished via a mercury lamp and quartz slide having a transparency of approximately 95%. The slide was placed at a 45° angle in front of the slit, while the mercury lamp was placed at 90° to the side of the entrance slit. This allowed 95% of the signal from the probe to be transmitted through the slide while 5% of the signal from the mercury lamp was reflected into the slit for calibration. Figure 2 illustrates the spectrometer setup.

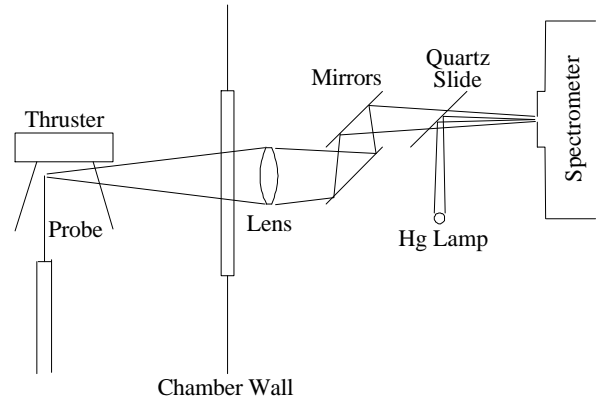


Figure 2. Spectrometer Setup

Thrust Stand

Thrust measurements were made on a NASA LeRC[4] type inverted ballistic pendulum thrust stand. This stand is nominally capable of a resolution of 0.5 mN but due to excessive vibrations from the cryopump and cold heads the resolution for these tests was approximately 3mN.

Quadruple probe

The quadruple probe used was based on the theory developed by Fife[11], which was an extension of the triple probe theory of Chen and Sekiguchi[12]. Unlike single and double probe techniques, the quadruple probe required no voltage sweep. This allowed nearly instantaneous measurements of electron temperature and number density, limited only by the ion plasma frequency[10]. The probe consisted of four electrodes; three electrodes formed a triple probe aligned parallel to the flow in a horizontal plane while the fourth was bent ninety degrees in the same plane and aligned perpendicular to the flow. Figure 3 illustrates the probe construction.

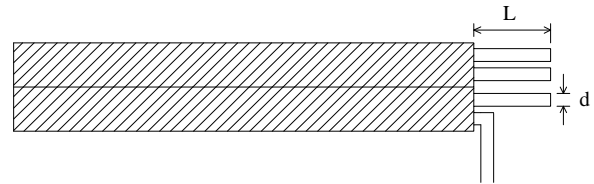


Figure 3. Side View of Quadruple Probe Electrode Configuration

Probe length, L , was 0.074 in. while the diameter, d , was 0.015 in. Representative values of electron number density and electron temperature in the SPT-70 plume fell in the range of 1×10^{11} to $1 \times 10^{12} \text{ cm}^{-3}$ and

1 to 6 eV respectively, with the upper limits occurring closer to the exit plane of the thruster. These values yielded a Debye length of $\lambda_d = 2 \times 10^{-5} \text{m}$. For a probe radius of $2 \times 10^{-4} \text{m}$, the ratio of probe radius to Debye length was 10, allowing the use of the thin sheath approximation. It followed from thin sheath theory that the ion current density was independent of probe potential and did not vary between electrodes.

All electrodes had the same dimensions but different effective collection areas due to the directed ion flux. The triple probe as a whole was floating and the relative potential of each electrode, including the fourth electrode, is shown in Figure 4. Figure 5 illustrates the circuit for the quadruple probe.

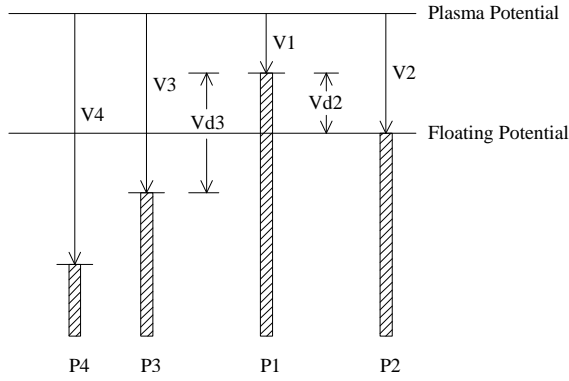


Figure 4. Relative Potentials of Quadruple Probe Electrodes

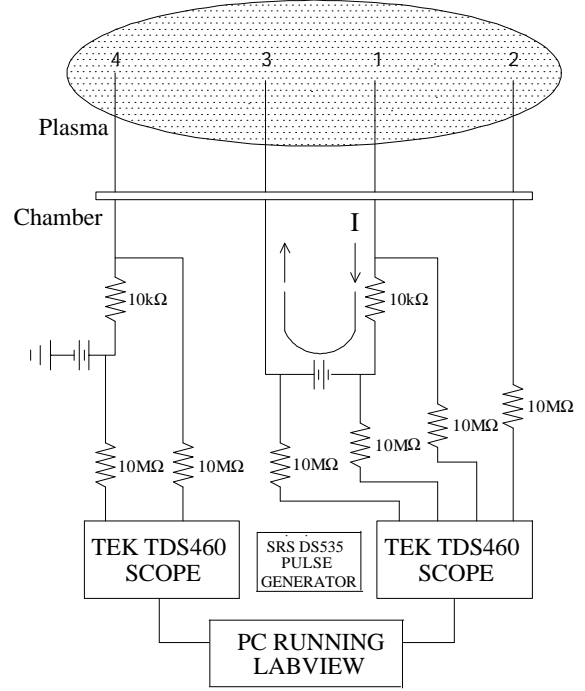


Figure 5 Quadruple Probe Circuit

With the previous assumptions, the following expression, containing only T_e as an unknown, was obtained[12]:

:

$$\frac{1}{2} = \frac{1 - \frac{A_3}{A_1} \exp(-c_{d2})}{1 - \exp(-c_{d3})}$$

(20)

where

$$c_{d2} = \frac{e|V_2 - V_1|}{k_b T_e}$$

(21)

and

$$c_{d3} = \frac{e|V_3 - V_1|}{k_b T_e}$$

(22)

In order to solve for the electron number density, one additional piece of information was needed. As pointed out earlier, the triple probe as a whole was floating, yielding no useful information on the electron saturation current and hence electron number density. Chen and Sekiguchi[12] solved this by modeling the ion sheath formation, assuming: 1) $T_e \gg T_i$, 2) a maxwellian electron energy distribution, and 3) a thin sheath. The ion current density was given by

$$J_i = \exp(-0.5)en_e \left(\frac{k_b T_e}{m_i} \right)^{1/2} \quad (23)$$

and the electron number density was then

$$n_e = \frac{\exp(0.5) \frac{I}{A_3}}{e \left(\frac{k_b T_e}{m_i} \right)^{1/2} (\exp(c_{d2}) - 1)} \quad (24)$$

One key assumption made by both Chen and Sekiguchi[12] and Tilley[10] in their application of the triple probe was that each electrode had the same surface area and, by extension, identical collection areas. In the case of the Hall thruster, each electrode had the same physical dimensions but different effective collection areas depending on their orientation to the directed ion flux. To account for this, Fife[11] added a fourth electrode oriented perpendicular to the flow. The collection area of this electrode was well defined, being simply the plane projected area of the probe, and it did not vary, as it was always perpendicular to the ion flow. Thus with the assumption that ion current density was the same to each probe, the effective collection area of a probe could then be determined by comparing the ion current of a given electrode to that of electrode 4.

$$A_i = A_4 \frac{I_i}{I_4} \quad (25)$$

Positioning System

The quadruple probe used in these experiments was mounted to a high speed reciprocating linear actuator. This actuator had a maximum speed of 50 in./s with an acceleration time constant of approximately 8ms.

The actuator was operated at its positive and negative physical limits only, using a Stanford Research Systems Model DS535 Pulse Generator to drive the actuator to its physical limit in one direction, pause for a specified period of time and then return to its opposite limit. The actuator had a stroke length of 2 inches with a transit time of approximately 150ms, estimated from the rate of change of probe traces recorded on a TEK TDS460 oscilloscope. All resident times given for the reciprocating probe include this transit time.

The reciprocating probe assembly was in turn mounted to a Parker 2-axis positioning table with a total travel of 12 inches in both directions but with a much slower speed than the actuator. This table was used to move the probe from a safety position well outside the thruster plume to the centerline of the discharge chamber, at the 9 o'clock position, and 2 inches downstream. This served as the home position for the reciprocating probe, which moved in an axial direction only, positioning the probe either at the exit plane or several millimeters upstream of the exit plane.

EXPERIMENTAL RESULTS

Spectra from the thruster is presented in Figure 6 for three cases: 1) baseline with the Hg lamp, thruster off and no probe, 2) thruster running and no probe, and 3) thruster running and the probe burning. Several additional species appeared with the probe burning, indicating that the presence of the probe was changing the composition and excitation state of the plasma in the neighborhood of the probe.

Variations of thruster parameters are shown in Figure 7. The probe reached a point approximately 3mm upstream of the exit plane at time $t=30s$. The parameters were all synchronized with the PMT signal indicating that changes corresponded directly with probe burning. The PMT light for this data was collected with the spectrometer grating rotated to achieve broadband reflection with no wavelength dispersion. Cathode potential and discharge current both changed significantly with the presence of the probe. The thrust also began to oscillate although the mean value appeared to remain constant. These initial experiments indicated that the probe had a significant effect on the thruster parameters when material was being ablated.

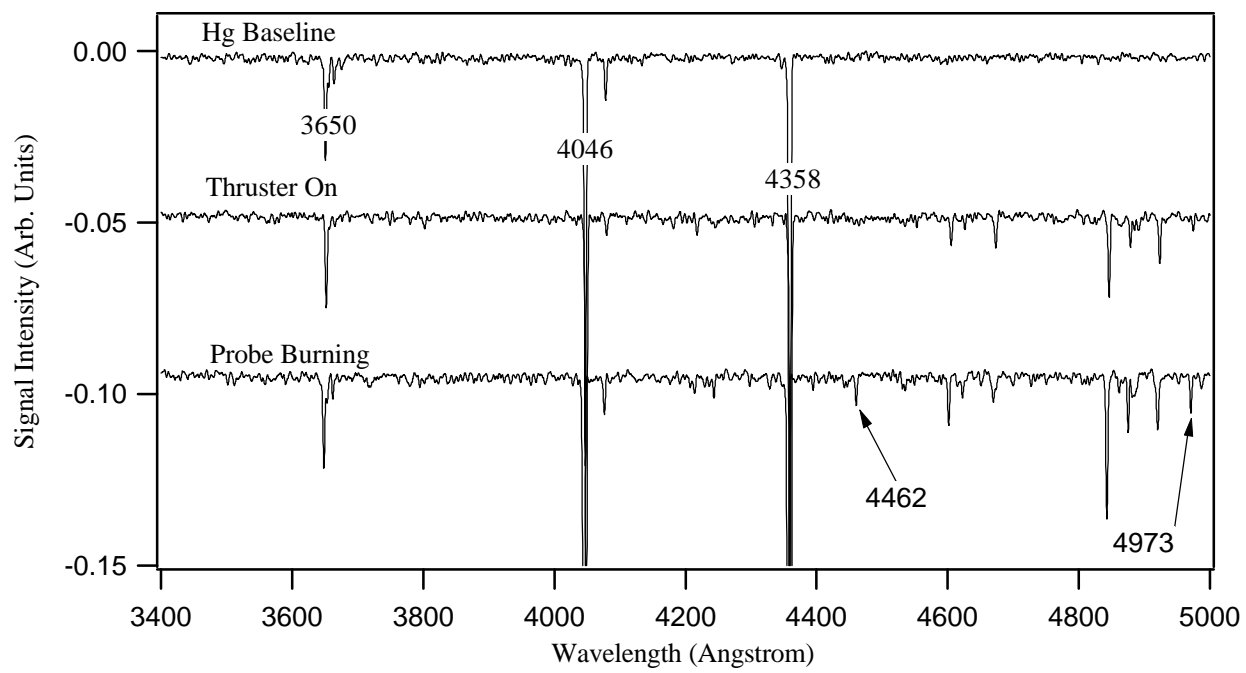


Figure 6. Spectra from Burning Probe

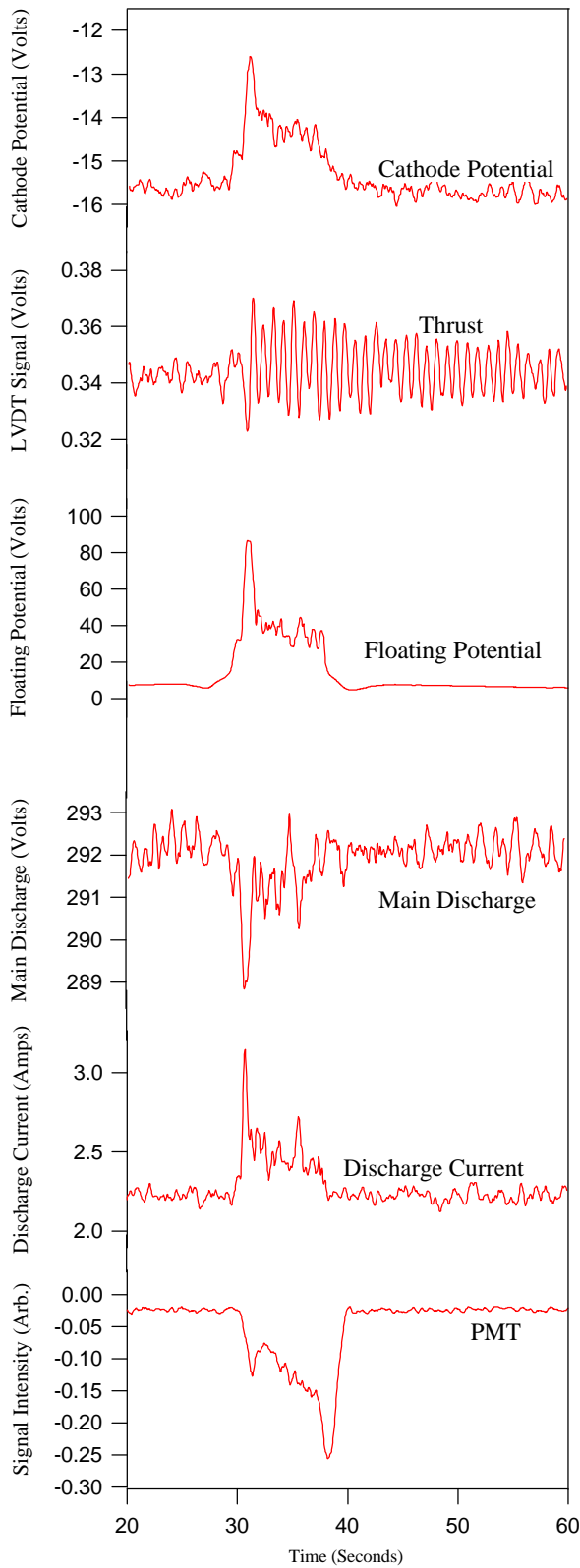


Figure 7. Thruster Operational Parameter Variations with Probe Burning .

The next phase of the experiments incorporated the reciprocating quadruple probe. From previous data, it was determined that the insulator material was burning almost immediately upon insertion into the discharge chamber while the tungsten would survive for several minutes. Therefore, a bare alumina tube was inserted into the thruster chamber with the quadruple probe placed approximately 5 inches laterally and 2 inches downstream of the alumina. Figure 8 illustrates the response from the probe.

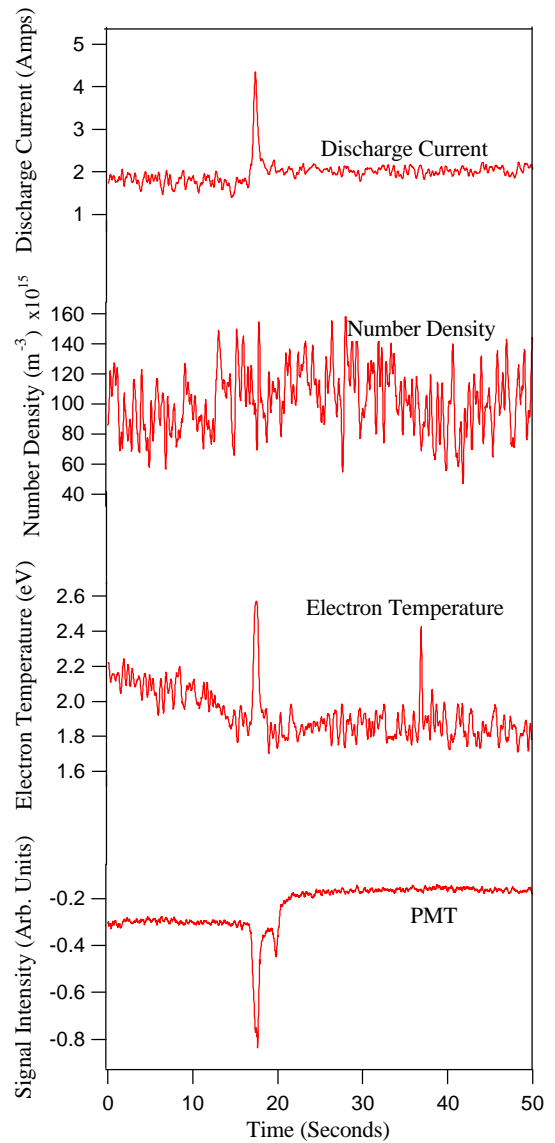


Figure 8. Local Plasma Parameter Variation Approx. 6'' From Burning Probe

As with the data of Figure 7, the response of the PMT coupled with the increase in discharge current indicated that insulator material was ablating. Electron number density remained relatively constant but electron temperature showed a definite spike corresponding to insulator burning. Note again that the probe measured these variations more than 5 inches away from the location of the burning probe.

As discussed earlier, the tungsten electrode did not reach a burning state for several minutes. However, significant changes in measured plasma parameters were observed long before the electrode reached a burning state. Figures 9 through 12 show the quadruple probe response as a function of time when it is positioned at the exit plane, allowing it to experience significant particle flux without burning. Local plasma parameters remained constant over the 0.5 second pulse but began to vary as the resident time at the exit plane exceeded 1 to 2 seconds. In particular, Figure 12 shows a 20% variation in electron temperature over a period of less than five seconds.

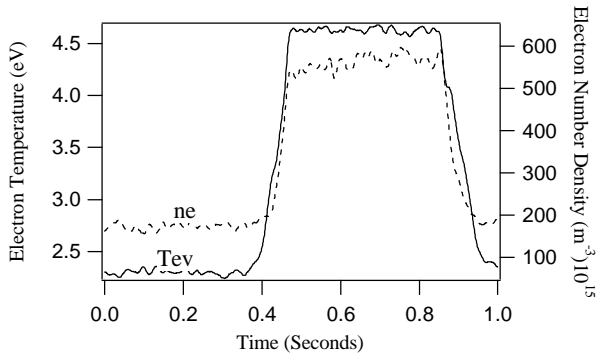


Figure 9. Electron Temperature and Number Density – 0.5s Pulse

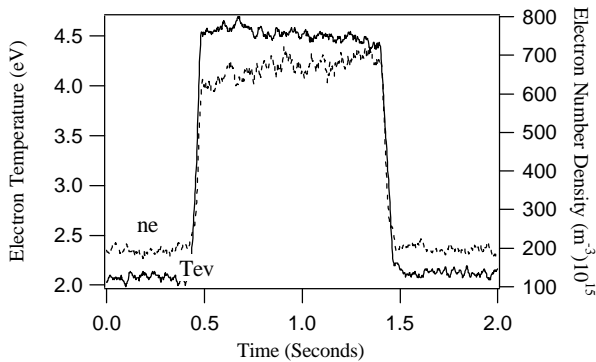


Figure 10. Electron Temperature and Number Density – 1s Pulse

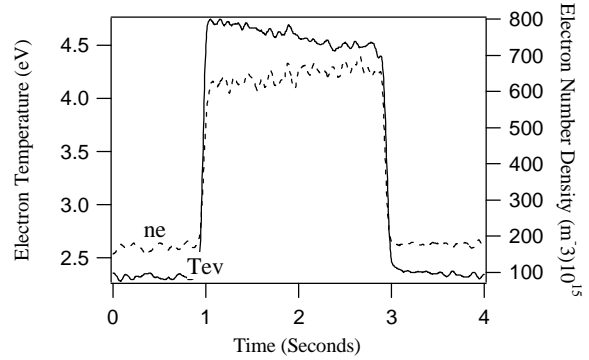


Figure 11. Electron Temperature and Number Density – 2s Pulse

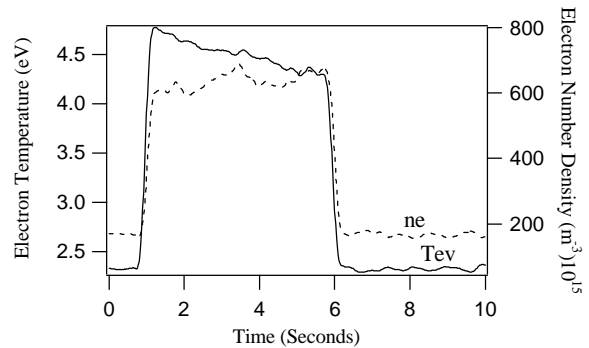


Figure 12. Electron Temperature and Number Density – 5s Pulse

Figures 13 and 14 show the cumulative effect of multiple reciprocations at the exit plane. Although plasma parameters remained constant over a half second pulse, the probe continued to be affected by the plasma flux during each successive insertion, eventually effecting measurements. The evolution of electron temperature and number density followed that for previous tests where the probe remained inserted.

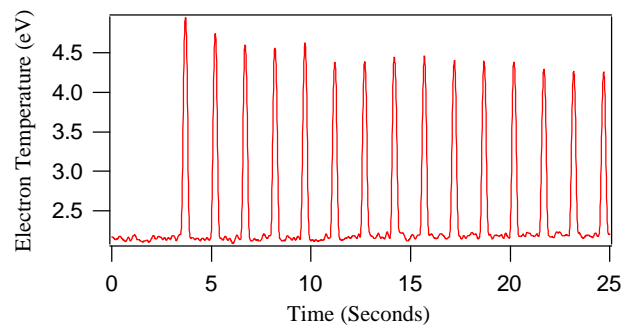


Figure 13 Electron Temperature Evolution for Multiple 0.5s Pulses at Exit Plane

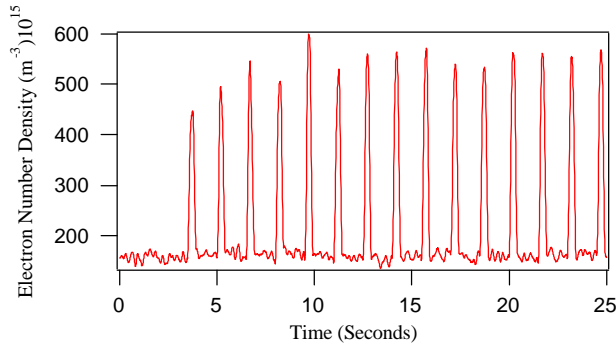


Figure 14 Electron Number Density Evolution for Multiple 0.5s Pulses at Exit Plane

This same experiment was performed with the probe inserted approximately 5mm into the discharge chamber where rapid burning was known to occur. Because of the rapid burning observed previously, a 0.5s pulse was used. Even for this short time scale, output from the PMT indicated the probe was burning. The probe survived three 0.5s pulses before a large amount of insulator material was ablated, exposing a section of the tungsten electrode.

DISCUSSION

The experimental results presented above illustrate the difficulties involved with the use of electrostatic probes. The data fell into two main sections. The first involved measurements outside the discharge chamber where particle flux was not sufficiently energetic to ablate probe material. In this region, probe lifetime was not an issue. However, as Figures 9-14 clearly illustrate, local plasma parameter measurements varied significantly over time periods on the order of seconds. One possibility is that the probe was contaminated. Contamination of electrostatic probes is a common problem and has been well documented[10]. In general, contamination in the form of resistive layers inhibits current collection resulting in artificially high electron temperatures. Experimental results presented here indicate an opposite trend with electron temperature decreasing over time. This may be explained by contaminants being cleaned by the directed particle flux rather than being deposited. Another possibility is that the electrical characteristics of the probe are changing as a function of material temperature.

The second set of data involved measurements in the interior of the discharge chamber where particle energies and/or densities caused significant material

ablation. In this case, not only were local measurements affected, but the operational characteristics of the thruster itself were significantly perturbed. Figures 6-8 illustrate this effect. These data were recorded over several seconds to illustrate probe ablation effects and to verify that the variations observed were not transient in nature. It is clear from Figure 7 that thruster perturbations occurred the entire time that the probe was burning. The high speed reciprocating probe was then employed in an attempt to probe the interior of the thruster on a short enough time scale so as not to ablate probe material and perturb the thruster. At the fastest probe speeds, material ablation was unavoidable.

Experiments ended when enough insulator material had been ablated to render the probe inoperable. Subsequent analysis of the probe revealed that the insulator had burned through, exposing a portion of one electrode. The failure point was limited to a small region approximately 1mm long, 1mm back from the tip, along the top of the probe. Figure 15 shows the failure point of the probe.

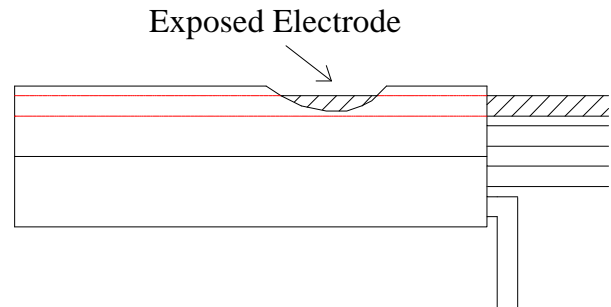


Figure 15. Damaged Probe

It is believed this burning pattern resulted from enhanced heating due to the Hall current. Using representative values for number density, magnetic field strength and electric field strength, the electron $E \times B$ drift velocity is approximately 2.5×10^6 m/s. This gives a power load from the electrons of 700 W/cm^2 . Using the bulk heating approach outlined in the theory section, the burning time of alumina is estimated to be 130ms. This is on the order of the transit time of the reciprocating probe, supporting experimental observations that the probe burn time is less than 0.5s inside the discharge chamber.

CONCLUSIONS

A high speed reciprocating probe system was assembled to investigate the effects of probe heating and material ablation on the operation of Hall thrusters and on the measurement of local plasma parameters. At the exit plane, no material ablation was observed, but the particle flux to the probe was sufficiently energetic to cause variations in the measurement of local plasma parameters. It was demonstrated that a high speed reciprocating probe could be used to avoid heating or contamination effects and make accurate measurements at the exit plane, with careful attention paid to total resident time.

In the interior of the discharge, however, severe disruptions in the Hall thruster operation were observed. This remained true even for time periods as short as 0.5s, the limit of the high speed probe system. Higher speeds or more robust insulators must be obtained if the entire interior plasma of the Hall thruster is to be successfully investigated.

ACKNOWLEDGEMENTS

The authors would like to extend their gratitude to their colleagues at the Air Force Research Laboratory for their invaluable assistance. Specifically, Mr. Jamie Malak for his help with all things electrical, without whose efforts this research could not have happened. The authors would also like to thank Mr. Mike Dulligan for his assistance in setting up and running the SPT-70 and Mr. Dave White for his help with the reciprocating probe system. Finally, the authors would also like to thank Lt. Jason LeDuc, Cpt. Richard Salasovich and Mr. Tom Byron for their many helpful insights and suggestions. Mr. James Haas is supported by the Air Force Palace Knight Program.

REFERENCES

1. Mott-Smith, H.M., Langmuir, I., Phys. Rev. 28 (1926) 727.
2. Rhodes, T.L., et. al., "Fast Reciprocating Probe System Used to Study Edge Turbulence on TEXT", Rev. Sci. Instrum., Vol. 61, No. 10, October 1990, pp. 3001-3003.
3. Seifert, W., et. al., "Methods for the Numerical Calculation of the Plasma Potential from Measured Langmuir Probe Characteristics", Contrib. Plasma Phys., Vol. 26, No. 4, 1986, pp. 237-254.
4. Marrese, C.M., et. al., "D-100 Performance and Plume Characterization on Krypton," AIAA 96-2969, July 1996.
5. Gallimore, A.D., et. al., "Near and Far-field Plume Studies of a 1 kW Arcjet," AIAA 94-3137, June 1994.
6. Kim, S-W., et. al., "Very-Near-Field Plume Study of a 1.35 kW SPT-100," AIAA 96-2972, July 1996
7. De Boer, P.T.C., "Electric Probe Measurements in the Plume of an Ion Thruster," Journal of Propulsion and Power, Vol. 12, No. 1, Jan.-Feb. 1996.
8. Burton, Rodney L., et. al., "Application of a Quadruple Probe Technique to MPD Thruster Plume Measurements," Journal of Propulsion and Power, Vol. 9, No. 5, Sept.-Oct. 1993
9. Guerrini, G., et. al., "Characterization of Plasma Inside the SPT-50 Channel by Electrostatic Probes," 25th International Electric Propulsion Conference, Cleveland, OH, Sept. 1997, IEPC 97-053.
10. Tilley, Dennis L., et. al., "The Application of the Triple Probe Method to MPD Thruster Plumes," AIAA 90-2667, July 1990.
11. Fife, J.M., et. al. "Analyzing Electron-Wall Interaction and Dynamic Response in Hall Thrusters," AIAA 98-3501, July 1998
12. Chen, S-L, and Sekiguchi, T., "Instantaneous Direct-Display System of Plasma Parameters by Means of a Triple Probe," Journal of Applied Physics, Vol. 36, No. 8, August 1965, pp. 2363-2375.